



HAL
open science

Modeling of isoamyl acetate production by fermentation with *Pichia fermentans* in an aerated system coupled to in situ extraction

Ana Karen Sánchez Castañeda, Violaine Athès, Marwen Moussa, Javier López Miranda, Jesús Bernardo Páez Lerma, Ioan Cristian Trelea

► **To cite this version:**

Ana Karen Sánchez Castañeda, Violaine Athès, Marwen Moussa, Javier López Miranda, Jesús Bernardo Páez Lerma, et al.. Modeling of isoamyl acetate production by fermentation with *Pichia fermentans* in an aerated system coupled to in situ extraction. *Process Biochemistry*, 2018, 65, pp.11-20. 10.1016/j.procbio.2017.10.010 . hal-01624572

HAL Id: hal-01624572

<https://hal.science/hal-01624572>

Submitted on 26 Oct 2017

HAL is a multi-disciplinary open access archive for the deposit and dissemination of scientific research documents, whether they are published or not. The documents may come from teaching and research institutions in France or abroad, or from public or private research centers.

L'archive ouverte pluridisciplinaire **HAL**, est destinée au dépôt et à la diffusion de documents scientifiques de niveau recherche, publiés ou non, émanant des établissements d'enseignement et de recherche français ou étrangers, des laboratoires publics ou privés.

**Modeling of isoamyl acetate production by fermentation with *Pichia fermentans*
in an aerated system coupled to *in situ* extraction**

Ana Karen Sánchez Castañeda^{a,b}, Violaine Athès^a, Marwen Moussa^a, Javier López Miranda^b, Jesús Bernardo Páez Lerma^b, Nicolás Óscar Soto Cruz^b; Ioan Cristian Trelea^{a*}.

^aUMR 782 Génie et Microbiologie des Procédés Alimentaires (GMPA), AgroParisTech, INRA, Université Paris-Saclay, F-78850, Thiverval-Grignon

^bTecnológico Nacional de México, Instituto Tecnológico de Durango, Departamento de Ingenierías Química-Bioquímicas. Blvd. Felipe Pescador 1830 Ote. Col Nueva Vizcaya. Durango, Dgo. 34080, México.

Authors e-mail: ana-karen.sanchez@inra.fr, violaine.athes-dutour@inra.fr, marwen.moussa@agroparistech.fr, jlopez@itdurango.edu.mx, jpaez@itdurango.edu.mx, nsoto@itdurango.edu.mx.

*Corresponding author:

Ioan Cristian Trelea

Tel: +33 1 30 81 54 90. Fax: +33 1 30 81 55 97.

E-mail address: cristian.trelea@agroparistech.fr

Abstract

This study deals with the production of isoamyl acetate (IAA) by fermentation of sugar cane molasses with the strain *Pichia fermentans* ITD00165, using L-leucine as precursor. A mathematical model that describes the experimental data from fermentation was developed for its use as a tool for further process optimization. The fermentation system was constantly aerated and coupled to liquid-liquid *in situ* extraction with decane as the recovery solvent. Thus, the model integrates the biological production of IAA, its partition coefficient in the two liquid phase system and the stripping effect of aeration. A productivity of 26-mg-L⁻¹h⁻¹ was obtained with addition of 4-g-L⁻¹ of L-leucine at 12-h of fermentation. The use of the model for process optimization was explored. According to it, the maximum theoretical productivity that can be obtained is 63-mg-L⁻¹h⁻¹. The model was used to determine that 1.6-g-L⁻¹ is the minimum concentration of L-leucine that can be added without significantly reducing IAA production. Also, it makes possible to propose an adequate decane/culture medium ratio, to have a desired final concentration and amount of recovered IAA. This value can be adjusted based on the needs of further purification steps and is useful to define a global economic optimum of the process.

Keywords: Aroma production, fermentation kinetics, partition coefficient, simulation, natural flavoring substance.

Chemical compounds studied in this article

Isoamyl acetate (PubChem CID: 31276); Decane (PubChem CID: 15600); L-leucine (PubChem CID: 6106).

1 **Introduction**

2 Esters of short-chain fatty acids are important flavor and fragrance compounds
3 widely used in the food and beverage industries. Isoamyl acetate (IAA) is
4 characterized by its strong smell of banana which gives it a very important place in
5 food, pharmaceutical and perfumery industries with a demand of 75 tons per year in
6 USA alone in 2010 [1–3], increasing over the years. This substance is obtained by
7 chemical synthesis, extraction from natural sources, or fermentation [4].

8 In recent years, the interest towards the production of flavor compounds through
9 white biotechnology processes over traditional methods has increased. Principal
10 reasons are that chemical synthesis often consists in an environmentally unfriendly
11 production process, with important drawbacks such as poor reactions selectivity
12 resulting in racemic mixtures, low yields, and high downstream costs [5,6]. Also,
13 consumers have developed an apprehensive attitude towards these synthetic
14 compounds, especially if the products are related to food or domestic usage.
15 Moreover, the extraction of flavoring compounds from natural sources gives very low
16 yields and has potential difficulties with obtaining the raw material [3,4,7]. Contrary
17 to chemical synthesis, flavors obtained by fermentation can have the “natural
18 flavoring substance” classification by the European (EC No 1334/2008) and U.S.
19 (21CFR101.22) regulations, which allows using them safely as an additive in food
20 and beverages. This has been the main reason for developing biochemical processes
21 over the years, but presently, after years of research, the inherent advantages of white
22 biotechnology processes are the driving force for its application: operation under mild

23 and more environmentally friendly conditions, as well as chemical and stereo
24 specificity of the obtained compounds, are the most important ones [8].

25 There are several published studies focused on IAA biological production. They
26 include enzymatic synthesis using lipases and esterases [1,3,9–15] and fermentation
27 process by microorganisms, especially yeasts strains [6,16–20]. Whole cell
28 fermentation can be a more economical method than enzymatic systems and easier to
29 scale up to industrial level. There are some encouraging studies with interesting IAA
30 productivities in the literature; for example, Yilmaztekin *et al.* [6] used a *Williopsis*
31 *saturnus* strain in a medium composed of beet molasses and fusel alcohols as a source
32 of isoamyl alcohol (IAOH), a precursor of the ester. A productivity of $2.46 \text{ mg L}^{-1} \text{ h}^{-1}$
33 was obtained by adding 1% of fusel alcohol at 72 h. Quilter *et al.* [19], obtained 1.16
34 $\text{mg L}^{-1} \text{ h}^{-1}$ using a mutant strain of *Saccharomyces cerevisiae* and testing several
35 fermentation conditions. However, these values are not high enough to make the
36 process attractive at industrial level and further optimization is needed.

37 In fermentative processes, the production of IAA is strongly affected by the medium
38 composition, fermentation conditions and the microorganism used [6,18,19].
39 However, a very important factor to consider is physical behavior of IAA in
40 fermentation medium once produced. IAA is a very volatile compound and its
41 production presents some difficulties including phase separation and challenging
42 product recovery. Moreover, IAA production could be favored by chemical
43 equilibrium shift through *in situ* extraction. A way to improve the performance of
44 fermentative processes is the direct recovery of the desired product, also called *In Situ*
45 Product Recovery (ISPR). This technique can overcome the inhibition by product

46 accumulation and also decreases the loss of cellular viability caused by product
47 toxicity [21,22]. Liquid-liquid extraction with organic solvents is a promising method
48 for IAA recovery, since IAA is more soluble in them than in aqueous solutions. For
49 the same reasons, lipase-catalyzed esterification is carried out in solvent systems
50 [12,14,15,23].

51 Modeling and simulation has become the most used tool for processes optimization,
52 since it makes possible to explore a wider range of parameter values at a minimum
53 price, compared to experimental approach. Thus, the aim of this work is to develop a
54 model able to describe the production and extraction of IAA from sugar cane
55 molasses, with L-leucine added as precursor, by fermentation with the strain *Pichia*
56 *fermentans* ITD00165. The model includes the behavior of IAA in an aerated
57 fermentation system coupled to an *in situ* extraction with a solvent (decane). As the
58 aeration factor affects the retention of IAA in the system due to a stripping effect, the
59 model is useful as an optimization tool to find the conditions in which the highest
60 amount of IAA could be produced and recovered.

61 **Materials and methods**

62 *1.1. Fermentations*

63 *1.1.1. Yeast strain*

64 The strain *Pichia fermentans* ITD00165 was used. It was one of the strains isolated
65 from a spontaneous fermentation of *Agave duranguensis* obtained from the Microbial
66 Biotechnology Lab's Culture Collection at the Durango Institute of Technology. It
67 was chosen because of its high IAA production capacity [24].

68 *1.1.2. Isoamyl acetate production*

69 Fermentations were carried out in 1 L glass containers with a diameter/height ratio of
70 1:2, where 600 mL of culture medium were inoculated with an initial concentration of
71 1×10^7 cells mL⁻¹ of a 24 h pre-grown culture. The pre-culture was inoculated in 100
72 mL of the sugar cane molasses medium in 250 mL Erlenmeyer flasks, with agitation
73 of 120 rpm at 28°C. In order to retain the IAA produced, 150 mL of decane (Sigma-
74 Aldrich, USA) was put at the top of the culture medium, creating an *in situ*
75 entrapping system. Compressed air was fed into the medium with a flow rate of 600
76 mL min⁻¹ (1 VVM) at the bottom of the vessel, in order to provide oxygen to the cells
77 and to agitate the culture medium. No other agitation system was used, thus liquid
78 phases were not mixed, only a slight local dispersion at liquid/liquid interface was
79 observed. The temperature was maintained at 28 °C and the fermentation was
80 monitored during 24 h. In fermentations, the effect of addition of the amino acid L-
81 leucine (Sigma-Aldrich, USA) as a precursor of IAA was tested. Therefore, three
82 experiments were carried out: 1) Fermentation with no addition of L-leucine, 2) The
83 addition of 4 g L⁻¹ of L-leucine at the beginning of fermentation (t_0) and 3) adding 4 g
84 L⁻¹ after 12 h of fermentation (t_{12}). All experiments were performed in duplicate.

85 *1.1.3. Process monitoring*

86 Samples of 1 mL of medium and decane phases were taken for 24 hours, every 4
87 hours for experiments 1 and 3, and every 2 hours for experiment 2. Monitoring
88 consisted in measurements of biomass by staining viable count with methylene blue
89 in a Neubauer chamber and dry weight; reducing sugars by DNS technique [25]; L-
90 leucine and the nitrogen (N) source in molasses by a colorimetric method with

91 ninhydrin [26]; and IAA production measured in the decane phase by gas
92 chromatography on a Gas Chromatograph 6890N (Agilent Technologies, USA)
93 equipped with a flame ionization detector (FID) and a HP-Innowax column (Hewlett-
94 Packard, USA) (length, 30 m; inside diameter, 0.25 mm; film thickness, 0.25 μm).
95 Temperatures were as used by Rojas *et al.*[20] with some modifications: injector
96 block and detector 220 and 300 $^{\circ}\text{C}$, respectively. The oven temperature was
97 programmed as follows: equilibrated at 60 $^{\circ}\text{C}$ for 10 min, followed by a ramp of 20 $^{\circ}\text{C}$
98 min^{-1} , up to 250 $^{\circ}\text{C}$. Ethanol and IAOH were analyzed in culture medium by gas
99 chromatography with a method designed for alcohols [27]: injector block and
100 detector 250 and 300 $^{\circ}\text{C}$, respectively; 1:10 split ratio; oven temperature equilibrated
101 at 40 $^{\circ}\text{C}$ for 5 min, followed by a ramp of 10 $^{\circ}\text{C min}^{-1}$, up to 260 $^{\circ}\text{C}$.

102 1.2. *Aeration effect on retention of isoamyl acetate in decane*

103 Experiments were carried out in the same conditions as fermentations but without cell
104 inoculation. Instead, IAA was added to the system at a concentration of 1 g L^{-1} in two
105 different conditions: 1) Adding IAA into the culture medium and 2) the same amount
106 of IAA was added into the decane phase. Samples of decane were taken periodically
107 and were analyzed by gas chromatography as mentioned before. All experiments
108 were performed in duplicate.

109 1.3. *Molasses medium analysis by HPLC*

110 A sample of fermentation medium, consisting in molasses diluted at 100 g L^{-1} with
111 distilled water was analyzed by HPLC in order to determine the sugars and
112 aminoacids content. Sugars were analyzed using a column Biorad Aminex with a

113 stationary phase of sulfonated divinyl benzene-styrene (HPX-87H, 300 mm x 7.8 mm
114 x 9 μ m), at a temperature of 35°C, UV detection was made at 210 nm. For
115 aminoacids, anAccQ-Fluor Reagent Kit was injected in a Waters column (ACCQ-
116 TAG, 150mm x 3.9 x 4 μ m), at a temperature of 34°C, and fluorescent UV detection
117 was made at 250 nm for excitation and 395 nm for emission.

118 1.4. Determination of partition coefficients

119 1.4.1. Gas-liquid partition coefficient (K_{gq})

120 The Phase Ratio Variation (PRV) method was used as described by Morakul *et al.*,
121 [28]. In order to evaluate the effect of the changes in medium composition during
122 fermentation, 8 different solutions of IAA at 1 g L⁻¹ were prepared in different
123 aqueous matrices, simulating different stages of fermentation during IAA production:
124 1) water, 2) sucrose 100 g L⁻¹, 3) ethanol 10 g L⁻¹, 4) sucrose 150 g L⁻¹, 5) ethanol 15
125 g L⁻¹, 6) sucrose 50 g L⁻¹ + ethanol 5 g L⁻¹, 7) sucrose 25 g L⁻¹ + ethanol 7.5 g L⁻¹, and
126 8) sugar cane molasses 100 g L⁻¹. These conditions were proposed considering a
127 maximum production of ethanol of 15 g L⁻¹ and a maximum sugar concentration of
128 100 g L⁻¹ in the fermentation medium during the process. Aliquots of 50 μ L to 2 mL
129 from each solution were introduced into four different headspace vials (22 mL,
130 Chromacol, France) closed with Teflon/silicone septa in metallic caps, giving volume
131 ratios between gas and liquid phases (β) of 10 to 439. The vials were then
132 equilibrated at 28°C for at least 1 h (the time required to reach equilibrium in static
133 conditions). Once equilibrium was reached, a 500 μ L sample of headspace gas was
134 taken with a gastight syringe, preheated to 40 °C, in an automatic headspace sampler
135 CTC Pal and injected with a 100 μ L s⁻¹ rate to a gas chromatograph (Agilent

136 G1530A, Germany) using FID detector. A HP-INNOWax column (30 m × 0.53 mm
137 × 1.00µm) from Agilent (stationary phase: polyethylene glycol) was used, using
138 helium as a carrier gas with a flow rate of 10 mL min⁻¹. The oven temperature started
139 at 60 °C followed by a ramp of 10 °C min⁻¹ up to 220 °C. Injector and FID detector
140 temperature was 250°C. Peaks areas were acquired with Agilent GC Chemstation
141 software. A mass balance equation was used for partition coefficients calculation, as
142 described by Ettre *et al.* [29].The gas-liquid partition coefficient for IAA was
143 expressed as the concentration ratio (K_{gq}):

$$K_{gq} = \frac{C_g^*}{C_q^*} \quad (1)$$

144 with C_g^* and C_q^* being IAA concentration at equilibrium in the gas and aqueous
145 phases respectively.

146 1.4.2. Liquid-liquid partition coefficient (K_{dq})

147 In this determination, different IAA solutions of 0.1 g L⁻¹ in aqueous phase were also
148 prepared changing the matrix composition in order to simulate the changes in the
149 medium during fermentation. The solutions were 1) water, 2) sucrose 100 g L⁻¹, 3)
150 ethanol 10 g L⁻¹, 4) sucrose 25 g L⁻¹ + ethanol 7.5 g L⁻¹, 5) sucrose 50 g L⁻¹ + ethanol
151 5 g L⁻¹, 6) sucrose 70 g L⁻¹ + ethanol 10 g L⁻¹, and 7) sugar cane molasses 100 g L⁻¹.
152 Some solutions had different sucrose and ethanol concentrations from those used in
153 the gas-liquid partition coefficient measurements (K_{gq}), in order to have intermediate
154 concentration values. Then, 25 mL of each solution were put in contact with 25 mL
155 of decane in 60 mL separation funnels. They were left to reach the equilibrium in
156 static conditions for at least 48 h at a temperature of 28°C.

157 After equilibrium was reached, 1.5 mL samples of aqueous and decane phase were
158 taken in 2 mL vials closed with Teflon/silicone septa in metallic caps and stored in
159 the tray at 4°C. A sample of 1 µL was taken from each vial with a water-tight syringe,
160 in an automatic headspace sampler CTC Pal and injected with a 5 µL s⁻¹ rate to the
161 gas chromatograph (G 1530A, Germany), equipped with the same column. For the
162 analysis method, oven temperature started at 35 °C followed by a ramp of 5°C min⁻¹
163 to 60 °C and another one of 15°C min⁻¹ up to 220 °C. Injector and FID detector
164 temperature was set to 250 °C.

165 IAA concentrations in both phases were determined using adequate calibration
166 curves. Partition coefficient K_{dq} was calculated as the ratio at equilibrium of IAA in
167 decane C_d^* and in aqueous solution C_q^* :

$$K_{dq} = \frac{C_d^*}{C_q^*} \quad (2)$$

168 *1.4.3. Statistical analysis*

169 Partition coefficient values were compared with a One Way Analysis of Variance
170 (ANOVA) and the Fisher Least Significant Difference (LSD) post-hoc test with the
171 program Statistica version 7.0 (StatSoft, USA).

172 *1.5. Dynamic model*

173 The equations of the mathematical model were implemented in a program written
174 under Matlab 2013b (The Mathworks Inc, Natick, MA). The parameters were
175 identified by linear and nonlinear regression, using the Statistic Toolbox.

176 *1.5.1. Modeling partition coefficients*

177 The values of gas-liquid and liquid-liquid partition coefficients were fitted to a
178 statistical model that accounts for dependence on the medium composition (at
179 constant temperature), as described by Mouret *et al.* [30]. Sugar and ethanol
180 concentrations, their interaction and the effect of molasses were considered:

$$\log K_{dq} = p_a + p_b S_t + p_c E + p_d S_t E + p_e M \quad (3)$$

$$\log K_{gq} = p_1 + p_2 S_t + p_3 E + p_4 S_t E + p_5 M \quad (4)$$

181 where K_{gq} and K_{dq} are the gas-liquid and liquid-liquid partition coefficients
182 respectively, E is the ethanol concentration (g L^{-1}), S_t is the sugar concentration (g L^{-1})
183 ¹), and M is the presence of molasses (0 or 1) in aqueous phase. Model parameters
184 $p_1 \dots p_5$ and $p_a \dots p_e$ are constants depending on the considered compound and
185 temperature, in this case IAA at 28°C. Parameter values were determined by stepwise
186 descending linear regression, starting with the complete model and removing
187 statistically not significant terms one by one, starting with the ones with the largest
188 coefficient of variation.

189 1.5.2. Modeling the isoamyl acetate loss in gas phase by stripping

190 IAA transfer in the system was considered as follows: it is transferred from the
191 aqueous medium (q), where it is synthesized by the cells, simultaneously to 1) the
192 decane phase (d); and 2) to the gas phase (g). Also, a fraction of the IAA in decane
193 phase is transferred to the gas phase. Medium and decane phases are very little
194 dispersed into each other, so the transfer to the gas phase is different in each liquid
195 phase. The IAA transferred to the air fed in the fermentation system was considered
196 as lost due to a stripping effect. Therefore, this could be described by the model

197 developed by Marin *et al.*[31] with some modifications (Equation 5), considering
 198 IAA present in both decane and fermentation medium, and the removal by the air
 199 flow passing through the system. The global mass balance between the liquids,
 200 namely decane (d) + aqueous medium (q) and the stripping gas (g) was written as:

$$\frac{d(C_d V_d + C_q V_q)}{dt} = -C_g \cdot Q_g \quad (5)$$

201 where C_d , C_q and C_g are IAA concentration in decane, aqueous and gas phase
 202 respectively, V_d and V_q are the volumes (mL) of decane and aqueous phase
 203 respectively, and Q_g is the air flow rate through the system (mL h⁻¹). It was assumed
 204 that the liquid and gas phases were not in equilibrium, and the expression of mass
 205 transfer from the two liquid phases (d , q) to the air flow (gas phase, g) is:

$$C_g \cdot Q_g = k_q A_q \left(C_q - \frac{C_g}{K_{gq}} \right) + k_d A_d \left(C_d - \frac{C_g}{K_{gd}} \right) \quad (6)$$

206 Here k_q and k_d are the overall mass transfer coefficients of IAA between the gas and
 207 the aqueous and decane phases respectively, and A_q and A_d are the interfacial areas
 208 of each phase with air bubbles [31]. K_{gd} is the partition coefficient between the gas
 209 and decane phases determined from Equations 1 and 2 according to Equation 7.

$$K_{gd} \stackrel{\text{def}}{=} \frac{C_g^*}{C_d^*} = \frac{K_{gq}}{K_{dq}} \quad (7)$$

210 At time scale of IAA production process by fermentation (12 h), equilibrium was
 211 considered between the aqueous phase and decane:

$$C_q = \frac{C_d}{K_{dq}} \quad (8)$$

212 After substituting C_q from Equation 8, equation 6 was solved for C_g , giving:

$$C_g = \frac{k_l a_l}{\left(D_g + \frac{k_l a_l}{K_{gd}}\right)} \cdot C_d \quad (9)$$

213 where

$$k_l a_l = \frac{\left(\frac{k_q A_q}{K_{dq}} + k_d A_d\right)}{V_q} \quad \text{and} \quad D_g = \frac{Q_g}{V_q} \quad (10)$$

214 The product $k_l a_l$ is a volumetric mass transfer coefficient which characterizes
 215 transfer between the liquid phase (decane + aqueous medium) as a whole and the gas
 216 phase and D_g is the specific aeration rate of the medium.

217 Substituting Equation 9 in 5, the loss rate of IAA, considering decane as the reference
 218 medium, is obtained:

$$\frac{dC_d}{dt} = - \frac{k_l a_l \cdot D_g}{\left(D_g + \frac{k_l a_l}{K_{gd}}\right) \left(\frac{V_d}{V_q} + \frac{1}{K_{dq}}\right)} \cdot C_d \quad (11)$$

219 Equation (11) can be solved easily assuming K_i , k_i , A_i and V_i to be constant in
 220 isothermal conditions, leading to Equation 12 that gives the residual concentration of
 221 IAA in decane considering the stripping effect of the air fed into the system:

$$C_d = C_{d0} \exp \left(- \frac{k_l a_l \cdot D_g}{\left(D_g + \frac{k_l a_l}{K_{gd}} \right) \left(\frac{V_d}{V_q} + \frac{1}{K_{dq}} \right)} t \right) \quad (12)$$

222

223 The only unknown parameter in this equation is the volumetric mass transfer
 224 coefficient ($k_l a_l$). In order to verify the assumption that liquid phases are not in
 225 equilibrium with the gas phase and IAA stripping is limited by mass transfer, a
 226 variant of the model considering equilibrium between the gas and the liquid phases
 227 was also considered for comparison, corresponding to a very large $k_l a_l$ value. In that
 228 situation, Equation 12 reduces to Equation 13:

$$C_d = C_{d0} \exp \left[-K_{gd} \cdot \frac{D_g}{\left(\frac{V_d}{V_q} + \frac{1}{K_{dq}} \right)} t \right] \quad (13)$$

229 1.6. Modeling the isoamyl acetate production by fermentation

230 To develop the fermentation model, the metabolic pathway involved in IAA synthesis
 231 by yeast was considered (Figure 1) [32]. IAA is formed from esterification of IA OH
 232 and the acetyl group from acetyl coenzyme A. Depending on medium composition,
 233 IA OH could be produced *de novo* from sugars consumption or by a catabolic
 234 pathway from degradation of the amino acid L-leucine, called Ehrlich pathway [33].
 235 The acetyl-CoA formed during metabolism comes mainly from sugar consumption
 236 and is used in several other reactions like biosynthesis of lipids, amino acids, fatty
 237 acids, and is also involved in the tricarboxylic acids cycle [32].

238 Table 1 shows the equations used to describe the production and consumption of the
239 compounds considered in the fermentation model, without considering extraction by
240 decane and losses by stripping. Biomass, ethanol, IAOH and IAA are the produced
241 compounds, while fermentable reducing sugar, L-leucine and IAOH as well, are the
242 consumed ones. To describe biomass production, the Monod equation was used
243 (Equations 14 and 20). In that case biomass production is proportional to fermentable
244 sugars consumption. Therefore, fermentable sugars consumption was described by
245 Equation 18, $Y_{X/S}$ being the yield of biomass production related to sugar
246 consumption. Ethanol production was also considered to be proportional to sugar
247 consumption (Equation 15), using the corresponding yield ($Y_{EtOH/S}$).

248 According to the metabolic pathway (Figure 1), IAOH is formed from both sugars
249 and L-leucine consumption, with the corresponding specific production rates ξ_S and
250 ξ_L and is consumed for IAA synthesis with yield $Y_{IAA/IAOH}$ (Equation 16). For IAA
251 production from IAOH, an analogous of the Monod equation was used, considering
252 both fermentable sugars and IAOH as limiting substrates (Equations 17 and 23). L-
253 leucine consumption is described by Equation 19, the specific consumption rate also
254 involving fermentable sugar as limiting substrate (Equation 22).

255 *1.6.1. Coupled model*

256 In order to represent the IAA retained in the fermentation system with decane and
257 stripping, the mass balance equation for IAA production from the fermentation model
258 (Equation 17) was modified to include IAA partition between the fermentation

259 medium and decane as well as IAA losses by stripping (Equation 11) leading to
260 equation 24:

$$\frac{dC_d}{dt} = \nu X \frac{V_q}{V_d + \frac{V_q}{K_{dq}}} - \frac{k_l a_l \cdot D_g}{\left(D_g + \frac{k_l a_l}{K_{gd}}\right) \left(\frac{V_d}{V_q} + \frac{1}{K_{dq}}\right)} C_d \quad (24)$$

261 The result was expressed in terms of IAA concentration in decane (assuming
262 equilibrium between fermentation medium and decane, Equation 8) because all
263 concentration measurements were performed in this phase.

264 **Results and discussion**

265 *1.7. Model development*

266 *1.7.1. Gas-liquid (K_{gq}) and liquid-liquid (K_{dq}) partition coefficients*

267 Figure 2 shows the K_{gq} values at different concentrations of ethanol and sucrose,
268 compounds that were chosen to simulate the medium composition during
269 fermentation. It can be observed that an increment on ethanol concentration increased
270 the solubility of the esters in the aqueous phase, decreasing their volatility. On the
271 other side, sugar concentration has a ‘salting out’ effect, increasing the volatility of
272 aroma compound. Thus, K_{gq} value tends to decrease during fermentation. The same
273 tendencies were observed in the work of Morakul *et al.* [28].

274 Figure 3 shows liquid-liquid partition coefficient (K_{dq}) values. As it can be observed,
275 changes in medium composition have a much stronger impact than on K_{gq} . Sugar
276 concentration has a higher “salting out” effect than on K_{gq} . In the case of molasses
277 solution, the K_{dq} value is significantly smaller than for model solutions. This could
278 be because in molasses other components such as lipids, amino acids or minerals are
279 present, which could affect more importantly the K_{dq} value.

280 Table 2 shows the parameter values obtained from the stepwise linear regression of
281 K_{gq} and K_{dq} with the different simulated medium compositions. Parameters that are
282 not significantly different from zero were iteratively removed from the model,
283 beginning with the factor with the highest coefficient of variation [30]. For K_{dq}
284 regression, ethanol and molasses had a significant effect. Sugar concentration
285 coefficient resulted not significant. Note that solutions prepared to represent

286 fermentation conditions were a mixture of ethanol and sugar, inversely correlated as
287 in a real fermentation medium, which makes it difficult to differentiate each effect.
288 Thus, the absence of sugar coefficient in Equation 3 does not necessarily mean that
289 there is no effect. In the K_{dq} equation, sugar effect could have been absorbed by the
290 ethanol coefficient. For example, in the work of Morakul *et al.* [34] the partition
291 coefficient equation is expressed only in terms of ethanol concentration but it
292 represents also sugar concentration in the medium, since they are inversely related in
293 fermentation conditions.

294 As it was expected, the concentration of molasses had an important effect in K_{dq}
295 model, but is negligible in K_{gq} model. These results show that complex medium
296 (molasses) composition has a stronger effect on K_{dq} than on K_{gq} . Identifying which
297 compounds of the molasses solution have significant effects on K_{dq} requires further
298 investigations.

299 1.7.2. Isoamyl acetate loss by air stripping

300 Figure 4 displays the experimental data obtained in stripping experiments after
301 adding IAA in aqueous and decane phase, together with model predictions.
302 Determination coefficient (R^2) values for both experiments were 0.913 and 0.996
303 respectively. In fermentation conditions, 2.5% of IAA per hour is lost due to aeration,
304 and the value of $k_l a_l$ coefficient that represents mass transfer from liquid to gas phase
305 was $0.0117 \pm 0.0003 \text{ h}^{-1}$ (fitted using Equation 12). The relatively low value of the
306 volumetric mass transfer coefficient $k_l a_l$ for isoamyl acetate corresponds to reduced
307 IAA losses by stripping from the considered device, a desired feature in this case.

308 Although aeration has an important effect on IAA loss from fermentation system,
309 Rojas *et al.* [20] observed that its production by non-*Saccharomyces* strains is
310 improved in highly aerobic culture conditions (shaking at 120 rpm), compared with
311 minimally aerobic conditions (without shaking). From all the strain tested, *Pichia*
312 *anomala* had the best IAA production and it had a 21 fold increase in aerobic
313 conditions. Also, Inoue *et al.* [35] reported a large amount of IAA produced by a
314 *Hansenula mrakii* strain in aerobic conditions.

315 For modeling purposes, it was assumed that decane and aqueous phase were in
316 equilibrium at the fermentation time scale. This assumption appears to be verified by
317 the experimental data shown in Figure 4. The experiment of IAA added into the
318 culture medium shows that after 1 h of aeration, IAA transferred into decane phase,
319 and in the following measurements a decrease of concentration due to aeration can be
320 observed. Thus, it appeared that within 1 h, equilibrium between the two phases was
321 reached.

322 Figure 4 also shows in dashed lines the calculated loss of IAA with the assumption
323 that liquid and gaseous phases are in equilibrium (Equation 13). IAA losses are
324 clearly overestimated, meaning that the equilibrium between gas and liquid phases is
325 far from being reached, probably because the residence time of the air bubbles fed in
326 the system is very short. This corroborates the assumption that the stripping
327 phenomenon due to air feed is limited by mass transfer between liquid and gas phase,
328 and validates the model built on that basis.

329 *1.7.3. Parameter estimation for the fermentation model*

330 Data obtained from fermentation experiments 1 (no addition of L-leucine) and 2
331 (addition of L-leucine at t_0) were used to calculate the fermentation model parameters
332 (Table 3), while experiment 3 was used for validation of the model. Initial conditions
333 were taken from experimental values. In case of L-leucine in experiments 1 and 3, the
334 initial value was obtained from HPLC analysis of molasses, showing that there was a
335 small amount of this aminoacid (0.01 g L^{-1}). However, this amount is too small to
336 explain the IAA production with no addition of L-leucine into the medium, meaning
337 that there must be a pathway from sugar consumption to IAA synthesis as described
338 by Piendl and Geiger [32] and considered in the model.

339 The maximum specific growth rate μ_{max} was calculated by linear regression of the
340 logarithm of biomass produced ($\log X$) versus time (t) values in the exponential
341 growth phase of fermentation. The value obtained ($\mu_{max} = 0.230 \pm 0.006 \text{ h}^{-1}$) is
342 somewhat lower than the ones found in other works dealing with yeast growth in
343 sugar cane molasses, where μ_{max} can vary from 0.24 - 0.45 h^{-1} due to the difference in
344 nutrient or inhibitor composition in molasses, ambient conditions and the yeast strain
345 used [36–38]. Yields values $Y_{X/S}$ and $Y_{EtOH/S}$ were calculated by linear regression of
346 biomass and ethanol concentrations respectively vs. reducing sugars concentration.
347 For $Y_{IAA/IAOH}$ value, the stoichiometric value $130/88$ was considered (ratio of IAA
348 and IAOH molecular weights). Values of ξ_{Smax} , ξ_{Lmax} , v_{max} , K_S and $Y_{IAOH/L}$ were
349 determined by fitting the model simultaneously to biomass, sugar, L-Leucine, IAOH
350 concentration measurements in the fermentation medium and IAA concentration
351 measurements in decane.

352 In the case of K_{SIA} , K_L and K_{IAOH} values, it was found that in a range from 0 to 0.05 g
353 L⁻¹ their value had a minor effect on the model predictions. It was not possible to
354 determine exact values for these parameters with the experimental data available,
355 because experiments were performed in batch mode and corresponding substrates
356 (sugar, L-leucine, IAOH) were rate limiting during too short time periods. These
357 parameters were thus fixed to 0.02 g L⁻¹. For K_S , a value of 6.41 ± 0.57 g L⁻¹ was
358 found. This value depends on numerous factors such as environmental conditions,
359 composition of the medium and the strain used, so the range of values found in the
360 literature is quite extensive. For example Das *et al.* [38] determined a K_S of 1.53g L⁻¹
361 in fermentation with *Pichia fermentans* in sugar cane bagasse extract, Ponce *et al.*
362 [37] determined a value of 4.1 g L⁻¹ for *Saccharomyces cerevisiae* in fermentation of
363 sugar cane molasses. However, the value obtained in the present study is higher than
364 the works mentioned before, which confirms that substrate limitation coefficients
365 cannot be reliably determined in batch fermentations. Other micronutrients might
366 become limiting before complete sugar exhaustion.

367 1.8. Model validation

368 Once all model parameters were determined, data obtained from Experiment 3
369 (addition of L-leucine at t_{12}) was used for model validation. Figure 5 shows the model
370 predictions compared to experimental data. In general, it was obtained a good
371 agreement for all considered compounds. Sugar consumption was quite well
372 described by the model ($R^2=0.986$). The amount of the fermentable sugars was taken
373 as a fixed fraction of the total sugar concentration present in molasses, determined as
374 35% in Experiments 1 and 2. Biomass and ethanol are produced proportionally to the

375 sugar consumption, in agreement with the modeling assumptions; ethanol production
376 was well described by the model ($R^2=0.977$). However, biomass is slightly
377 underestimated by about 13% ($R^2=0.917$), which means that the growth rate μ_{max}
378 and yield $Y_{X/S}$ values were slightly higher in Experiment 3 than in Experiments 1 and
379 2.

380 Figure 5 shows that before 12 h of fermentation, IAOH was produced from sugars at
381 a low specific rate ξ_S , and almost entirely converted to IAA. After L-leucine addition,
382 the production rate of IAOH increased significantly since the Ehrlich pathway
383 participated to the synthesis with a higher specific rate ξ_L . This is consistent with
384 parameter values reported in Table 3, where $\xi_{Lmax} > \xi_{Smax}$. Most of IAOH produced
385 was converted to IAA at a specific rate v , which is consistent with $v_{max} > \xi_{Lmax}$ in
386 Table 3. However, it can be observed that there is a fraction of IAOH accumulated in
387 the fermentation medium, also described by the model ($R^2=0.819$).

388 IAOH accumulation is an important point to pay attention, since it has been proved
389 that this compound has an inhibitory effect on yeast cells growth. *Saccharomyces*
390 *cerevisiae* growth is slower at a concentration of about 4 g L^{-1} [39,40]; and *Williopsis*
391 *saturnus* growth is inhibited at concentrations of fusel oil greater than 2% (about 8 g
392 L^{-1} of IAOH). In this study, IAOH concentration determined in all the experiments
393 was less than 0.74 g L^{-1} , a small value compared to those found in the literature. This
394 is an advantage of maintaining a low IAA concentration in fermentation medium by
395 ISPR, which accelerates IAOH esterification, reducing its accumulation.

396 The accumulation of IAA was quite well described by the model ($R^2=0.952$) which
397 also calculated its actual production without losses by stripping (Figure 5). Model
398 calculations indicate an amount of about 17% of IAA lost by stripping in these
399 fermentation conditions. The highest IAA productivity obtained in experimental
400 conditions was $26 \text{ mg L}^{-1} \text{ h}^{-1}$ with addition of 4 g L^{-1} of L-leucine at 12 h of
401 fermentation, which is higher than other values reported in the literature obtained by
402 yeast fermentation without *in situ* extraction [6,41].

403 1.9. *Improvement strategies for isoamyl acetate production and retention*

404 The developed model can be used as a tool to simulate the process of IAA production
405 in different conditions in order to find those that results in a better IAA production
406 and retention, with a more efficient use of L-leucine and decane. Key conditions that
407 can be modified in order to improve production and retention in the system are: i) the
408 time and amount of L-leucine addition, and ii) the decane to culture medium volume
409 ratio in fermentation system.

410 L-leucine was added to the medium at a concentration of 4 g L^{-1} , however,
411 experimental data shows that it was not completely consumed by the cells, either
412 added from the beginning of fermentation or after 12 h. The model was used to test
413 different initial concentrations of L-leucine and simulate resulting IAA concentration
414 in decane. It was found that at concentrations of 1.6 g L^{-1} of L-leucine or higher, the
415 IAA final concentration is not significantly different from IAA production with 4 g L^{-1}
416 of L-leucine, as shown in Figure 6.

417 Figure 7a shows IAA distribution in the fermentation-extraction system at different
418 decane/medium ratios. It can be observed that the amount of IAA recovered in decane
419 phase increases by increasing the decane volume, as one may expect. A better
420 extraction percentage from the fermentation medium and lower losses by air stripping
421 are obtained. Although the amount of product retained increases with the amount of
422 decane used, final concentration of IAA tends to decrease as shown in Figure 7b,
423 which means obtaining an increasingly diluted solution and higher costs of
424 subsequent product purification. The model is thus a useful decision making tool to
425 determine the appropriate amount of decane, taking into account losses, the retained
426 IAA fraction and the type of downstream process to be used for purification. In order
427 to have an idea of the maximum potential production of the process, a simulation was
428 performed with a very high decane to culture medium ratio (100:1), assuming that
429 there will be no significant IAA loss in this condition. According to the model, with
430 1.6 g L^{-1} of L-leucine one can obtain a maximum theoretical productivity of 63 mg L^{-1}
431 h^{-1} , based on IAA recovered in decane data. The actual value of solvent/medium
432 ratio has to be selected considering the need for further purification steps. The model
433 is thus a useful tool to perform an economic evaluation of the process, in order to
434 optimize costs.

435 **Conclusion**

436 A model able to describe isoamyl acetate (IAA) production from sugar cane molasses
437 and L-leucine as precursor, by the strain *Pichia fermentans* ITD00165 was developed
438 and successfully used to predict the ester production indifferent conditions. It
439 reproduces quite well the coupled phenomena of the *in situ* production/extraction
440 process, and allows identifying the key points that can be improved to increase
441 production. The *in situ* extraction with decane resulted in several advantages: it
442 increased IAA production by decreasing product inhibition and IAOH accumulation
443 in the medium, which has been proven to inhibit yeast cell growth. Decane had a
444 good biocompatibility with the strain used. Moreover, it has a good affinity with IAA
445 which is very volatile and poorly soluble in water, so it decreased the loss of IAA by
446 stripping. In addition, thanks to the model it is easier to monitor IAA production from
447 a single measurement in the decane phase and to calculate the total amount produced.

448 The model describes not only the biological production of IAA, but also includes the
449 physical distribution of the ester according to key factors, like aeration, medium
450 composition changes through fermentation and volume ratio of both liquid phases. It
451 provides a more complete panorama of the process, allowing to test different
452 configurations and find the best compromise between fermentation conditions and
453 IAA retention to get the highest possible amount of product at acceptable purification
454 costs.

455 Further investigation is needed in order to better understand the whole process. For
456 example, aeration is a very important factor for IAA production, but it also increases

457 the loss by stripping, so it is a key process factor that has to be controlled. The
458 developed model is able to determine the rate of isoamyl acetate loss due to aeration,
459 and it could be further extended to include the effect of different air flow rates on
460 IAA production and thus indicate the best compromise. After testing model
461 predictions in a wide range of situations of practical interest, its implementation in
462 industrial processes could make it a valuable tool for process optimization and
463 provide a solid basis for choosing and developing a suitable product recovery
464 strategy.

465

Nomenclature		Units
A	Gas-liquid contact area	cm^2
C	Isoamyl acetate concentration	g L^{-1}
D_g	Specific aeration rate of the medium	h^{-1}
$EtOH$	Ethanol concentration	g L^{-1}
$IAOH$	Isoamyl alcohol concentration	g L^{-1}
K_{dq}	Liquid-liquid partition coefficient	g g^{-1}
K_{gq}	Gas-liquid partition coefficient	g g^{-1}
K_{IAOH}	Isoamyl alcohol saturation coefficient for isoamyl acetate production	g L^{-1}
K_L	L-Leucine saturation coefficient for isoamyl alcohol production	g L^{-1}
K_S	Sugar saturation coefficient for biomass production	g L^{-1}
K_{SIA}	Sugar saturation coefficient for isoamyl alcohol production	g L^{-1}
k_d	Overall mass transfer coefficient of isoamyl acetate between the decane and gas phase	cm h^{-1}
k_q	Overall mass transfer coefficient of isoamyl acetate between the aqueous and gas phase	cm h^{-1}
$k_l a_l$	Volumetric mass transfer coefficient between both liquid	h^{-1}

	phases as a whole and the gas phase	
L	L-leucine concentration	g L^{-1}
$p_1 \dots p_5$	Parameters of isoamyl acetate K_{dq} model	-
$p_a \dots p_e$	Parameters of isoamyl acetate K_{gq} model	-
Q_g	Aeration flowrate	mL h^{-1}
S	Sugar concentration	g L^{-1}
X	Biomass concentration	g L^{-1}
$Y_{EtOH/S}$	Ethanol yield per sugar consumption	g g^{-1}
$Y_{IAA/IAOH}$	Isoamyl acetate yield per isoamyl alcohol consumption	g g^{-1}
$Y_{IAOH/L}$	Isoamyl alcohol yield per L-leucine consumption	g g^{-1}
$Y_{X/S}$	Biomass yield per sugar consumption	g g^{-1}
μ_{max}	Maximum specific cellular growth rate	h^{-1}
ν_{max}	Maximum specific isoamyl acetate production rate	h^{-1}
ξ_{Lmax}	Maximum specific isoamyl alcohol production rate (from L-leucine)	h^{-1}
ξ_{Smax}	Maximum specific isoamyl alcohol production rate (from sugars)	h^{-1}

<i>Subscripts</i>	
d	Decane phase
g	Gas phase
q	Aqueous phase
f	Fermentable
t	Total
0	Initial value
*	Value at equilibrium
<i>Abbreviations</i>	
IAA	Isoamyl acetate

466

467

468

469 **REFERENCES**

470 [1] S. Torres, M.D. Baigorí, S.L. Swathy, A. Pandey, G.R. Castro, Enzymatic
471 synthesis of banana flavour (isoamyl acetate) by *Bacillus licheniformis* S-86 esterase,
472 Food Res. Int. 42 (2009) 454–460.

473 [2] W. Osorio-Viana, H.N. Ibarra-Taquez, I. Dobrosz-Gómez, M.Á. Gómez-
474 García, Hybrid membrane and conventional processes comparison for isoamyl acetate
475 production, Chem. Eng. Process. 76 (2014) 70–82.

476 [3] N. Mhetras, S. Patil, D. Gokhale, Lipase of *Aspergillus niger* NCIM 1207: A
477 Potential Biocatalyst for Synthesis of Isoamyl Acetate, Indian J Microbiol. 50 (2010)
478 432–437.

479 [4] M. Asunción, M. Sanromán, Production of Food Aroma Compounds:
480 Microbial and Enzymatic Methodologies, Food Technol Biotechnol. (2006) 335–353.

481 [5] N. Ben Akacha, M. Gargouri, Microbial and enzymatic technologies used for
482 the production of natural aroma compounds: Synthesis, recovery modeling, and
483 bioprocesses, Food Bioprod. Process. 94 (2015) 675–706.
484 doi:10.1016/j.fbp.2014.09.011.

485 [6] M. Yilmaztekin, H. Erten, T. Cabaroglu, Enhanced production of isoamyl
486 acetate from beet molasses with addition of fusel oil by *Williopsis saturnus* var.
487 saturnus, Food Chem. 112 (2009) 290–294.

488 [7] U. Krings, R.G. Berger, Biotechnological production of flavours and
489 fragrances, Appl Microbiol Biotechnol. 49 (1998) 1–8.

- 490 [8] J. Schrader, M.M.W. Etschmann, D. Sell, J.-M. Hilmer, J. Rabenhorst,
491 Applied biocatalysis for the synthesis of natural flavour compounds – current
492 industrial processes and future prospects, *Biotechnol. Lett.* 26 (2004) 463–472.
493 doi:10.1023/B:BILE.0000019576.80594.0e.
- 494 [9] M. Cyjetko, J. Vorkapić-Furač, P. Žnidaršič-Plazl, Isoamyl acetate synthesis
495 in imidazolium-based ionic liquids using packed bed enzyme microreactor, *Process*
496 *Biochem.* 47 (2012) 1344–1350. doi:10.1016/j.procbio.2012.04.028.
- 497 [10] M.J. Eisenmenger, J.I. Reyes-De-Corcuera, Enhanced synthesis of isoamyl
498 acetate using an ionic liquid–alcohol biphasic system at high hydrostatic pressure, *J.*
499 *Mol. Catal. B Enzym.* 67 (2010) 36–40. doi:10.1016/j.molcatb.2010.07.002.
- 500 [11] E. Fehér, V. Illeová, I. Kelemen-Horváth, K. Bélafi-Bakó, M. Polakovič, L.
501 Gubicza, Enzymatic production of isoamyl acetate in an ionic liquid–alcohol biphasic
502 system, *J. Mol. Catal. B Enzym.* 50 (2008) 28–32.
503 doi:10.1016/j.molcatb.2007.09.019.
- 504 [12] S.H. Krishna, S. Divakar, S.. Prapulla, N.. Karanth, Enzymatic synthesis of
505 isoamyl acetate using immobilized lipase from *Rhizomucor miehei*, *J. Biotechnol.* 87
506 (2001) 193–201. doi:10.1016/S0168-1656(00)00432-6.
- 507 [13] M.D. Romero, L. Calvo, C. Alba, A. Daneshfar, H.S. Ghaziaskar, Enzymatic
508 synthesis of isoamyl acetate with immobilized *Candida antarctica* lipase in n-hexane,
509 *Enzyme Microb. Technol.* 37 (2005) 42–48. doi:10.1016/j.enzmictec.2004.12.033.

- 510 [14] M.D. Romero, L. Calvo, C. Alba, M. Habulin, M. Primožič, ž. Knez,
511 Enzymatic synthesis of isoamyl acetate with immobilized *Candida antarctica* lipase
512 in supercritical carbon dioxide, *J. Supercrit. Fluids.* 33 (2005) 77–84.
513 doi:10.1016/j.supflu.2004.05.004.
- 514 [15] P. Žnidaršič-Plazl, I. Plazl, Modelling and experimental studies on lipase-
515 catalyzed isoamyl acetate synthesis in a microreactor, *Process Biochem.* 44 (2009)
516 1115–1121. doi:10.1016/j.procbio.2009.06.003.
- 517 [16] T. Asano, T. Inoue, N. Kurose, N. Hiraoka, S. Kawakita, Improvement of
518 Isoamyl Acetate Productivity in Sake Yeast by Isolating Mutants Resistant to
519 Econazole, *J. Biosci. Bioeng.* 87 (1999) 697–699.
- 520 [17] K. Hirooka, Y. Yamamoto, N. Tsutsui, T. Tanaka, Improved production of
521 isoamyl acetate by a sake yeast mutant resistant to an isoprenoid analog and its
522 dependence on alcohol acetyltransferase activity, but not on isoamyl alcohol
523 production, *J. Biosci. Bioeng.* 99 (2005) 125–129. doi:10.1263/jbb.99.125.
- 524 [18] C. Plata, J.C. Mauricio, C. Millán, J.M. Ortega, Influence of glucose and
525 oxygen on the production of ethyl acetate and isoamyl acetate by a *Saccharomyces*
526 *cerevisiae* strain during alcoholic fermentation, *World J. Microbiol. Biotechnol.* 00
527 (2004) 1–7.
- 528 [19] M.G. Quilter, J.C. Hurley, F.J. Lynch, M.G. Murphy, The production of
529 isoamyl acetate from amyl alcohol by *Saccharomyces cerevisiae*, *J. Inst. Brew.* 109
530 (2003) 34–40.

- 531 [20] V. Rojas, J.V. Gil, F. Piñaga, P. Manzanares, Studies on acetate ester
532 production by non-*Saccharomyces* wine yeasts, *Int. J. Food Microbiol.* 70 (2001)
533 283–289.
- 534 [21] T. Lamer, H.E. Spinnler, I. Souchon, A. Voilley, Extraction of benzaldehyde
535 from fermentation broth by pervaporation, *Process Biochem.* 31 (1996) 533–542.
536 doi:10.1016/0032-9592(95)00098-4.
- 537 [22] A. Freeman, J.M. Woodley, M.D. Lilly, In Situ Product Removal as a Tool for
538 Bioprocessing, *Nat Biotech.* 11 (1993) 1007–1012. doi:10.1038/nbt0993-1007.
- 539 [23] S.H. Krishnaa, B. Manoharb, S. Divakara, S.G. Prapullaa, N.G. Karanth,
540 Optimization of isoamyl acetate production by using immobilized lipase from *Mucor*
541 *miehei* by response surface methodology, *Enzyme Microb. Technol.* 26 (2000) 131–
542 136.
- 543 [24] G. Hernández-Carbajal, O.M. Rutiaga-Quiñones, A. Pérez-Silva, G. Saucedo-
544 Castañeda, A. Medeiros, C.R. Soccol, N.Ó. Soto-Cruz, Screening of native yeast
545 from *Agave duranguensis* fermentation for isoamyl acetate production, *Braz. Arch.*
546 *Biol. Technol.* 56 (2013) 357–363. doi:10.1590/S1516-89132013000300002.
- 547 [25] G.L. Miller, R. Blum, W.E. Glennon, A.L. Burton, Measurement of
548 carboxymethylcellulase activity, *Anal. Biochem.* 1 (1960) 127–132.
- 549 [26] S. Yokoyama, J.-I. Hiramatsu, A Modified Ninhydrin Reagent Using Ascorbic
550 Acid Instead of Potassium Cyanide, *J. Biosci. Bioeng.* 95 (2003) 204–205.
- 551 [27] Agilent Technologies, Agilent J&W. GC Column Selection Guide, (2007).

- 552 [28] S. Morakul, V. Athes, J.-R. Mouret, J.-M. Sablayrolles, Comprehensive Study
553 of the Evolution of Gas-Liquid Partitioning of Aroma Compounds during Wine
554 Alcoholic Fermentation, *J. Agric. Food Chem.* 58 (2010) 10219–10225.
- 555 [29] L. Ettre, C. Welter, B. Kolb, Determination of gas-liquid partition coefficients
556 by automatic equilibrium headspace-gas chromatography utilizing the phase ratio
557 variation method, *Chromatographia.* (1993) 73–84.
- 558 [30] J.R. Mouret, V. Farines, J.M. Sablayrolles, I.C. Trelea, Prediction of the
559 production kinetics of the main fermentative aromas in winemaking fermentations,
560 *Biochem. Eng. J.* 103 (2015) 211–218. doi:10.1016/j.bej.2015.07.017.
- 561 [31] M. Marin, I. Baek, A.J. Taylor, Volatile Release from Aqueous Solutions
562 under Dynamic Headspace Dilution Conditions, *J. Agric. Food Chem.* 47 (1999)
563 4750–4755.
- 564 [32] A. Piendl, E. Geiger, Technological factors in the formation of esters during
565 fermentation, *Brew. Dig.* 55 (1980) 26–35.
- 566 [33] S. Derrick, P.J. Large, Activities of the enzymes of the Ehrlich pathway and
567 formation of branched-chain alcohols in *Saccharomyces cerevisiae* and *Candida*
568 *utilis* grown in continous cuture on valine or amonium as sole nitrogen source, *J.*
569 *Gen. Microbiol.* 139 (1993) 2783–2792.
- 570 [34] S. Morakul, J.-R. Mouret, P. Nicolle, I.C. Trelea, J.-M. Sablayrolles, V. Athes,
571 Modelling of the gas–liquid partitioning of aroma compounds during wine alcoholic

572 fermentation and prediction of aroma losses, *Process Biochem.* 46 (2011) 1125–1131.
573 doi:10.1016/j.procbio.2011.01.034.

574 [35] Y. Inoue, S. Trevanichi, K. Fukuda, S. Izawa, Y. Wakai, A. Kimura, Roles of
575 Esterase and Alcohol Acetyltransferase on Production of Isoamyl Acetate in
576 *Hansenula mrakii*, *J. Agric. Food Chem.* 45 (1997) 644–649. doi:10.1021/jf960648o.

577 [36] A. Dourado, G. Goma, U. Albuquerque, Y. Sevely, Modeling and static
578 optimization of the ethanol production in a cascade reactor. I. Modeling, *Biotechnol.*
579 *Bioeng.* 29 (1987) 187–194. doi:10.1002/bit.260290208.

580 [37] G.H.S.F. Ponce, J. Moreira Neto, S.S. De Jesus, J.C. de C. Miranda, R. Maciel
581 Filho, R.R. de Andrade, M.R. Wolf Maciel, Sugarcane molasses fermentation with in
582 situ gas stripping using low and moderate sugar concentrations for ethanol
583 production: Experimental data and modeling, *Biochem. Eng. J.* 110 (2016) 152–161.
584 doi:10.1016/j.bej.2016.02.007.

585 [38] D. Das, D. Charumathi, N. Das, Combined effects of sugarcane bagasse
586 extract and synthetic dyes on the growth and bioaccumulation properties of *Pichia*
587 *fermentans* MTCC 189, *J. Hazard. Mater.* 183 (2010) 497–505.
588 doi:10.1016/j.jhazmat.2010.07.051.

589 [39] C. Martinez-Anaya, In yeast, the pseudohyphal phenotype induced by isoamyl
590 alcohol results from the operation of the morphogenesis checkpoint, *J. Cell Sci.* 116
591 (2003) 3423–3431. doi:10.1242/jcs.00634.

592 [40] K. Kern, C. Nunn, A. Pichova, J. Dickinson, Isoamyl alcohol-induced
593 morphological change in involves increases in mitochondria and cell wall chitin
594 content, FEMS Yeast Res. 5 (2004) 43–49. doi:10.1016/j.femsyr.2004.06.011.

595 [41] M.G. Quilter, J.C. Hurley, F.J. Lynch, M.G. Murphy, The production of
596 isoamyl acetate from amyl alcohol by *Saccharomyces cerevisiae*, J. Inst. Brew. 109
597 (2003) 34–40.

598

599 **Figure legends**

600 **Figure 1.** Schematic representation of the metabolic pathways involved in isoamyl
601 acetate synthesis [32].

602 **Figure 2.** Gas-aqueous phase partition coefficient (K_{gq}) values of isoamyl acetate for
603 different fermentation medium compositions. Error bars represent standard deviation
604 ($n = 2$), different letters correspond to significantly different values.

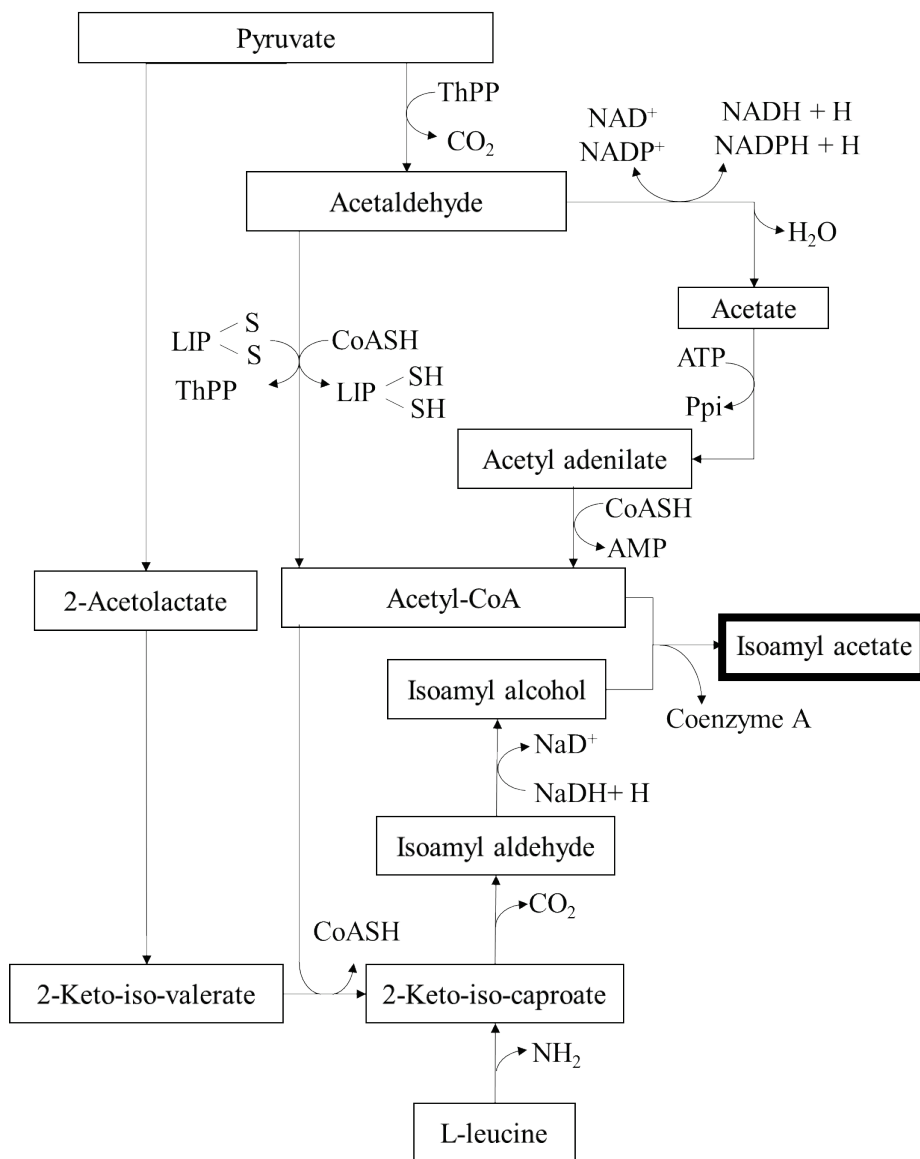
605 **Figure 3.** Decane–aqueous phase partition coefficient (K_{dq}) values of isoamyl acetate
606 for different fermentation medium compositions. Error bars represent standard
607 deviation ($n=2$), different letters correspond to significantly different values.

608 **Figure 4.** Isoamyl acetate stripping due to air flow. Symbols correspond to
609 experimental measurements and error bars represent standard error ($n = 2$). Solid
610 lines represent model predictions considering gas-liquid mass transfer resistance;
611 dashed lines represent model predictions assuming gas and liquid phases in
612 equilibrium.

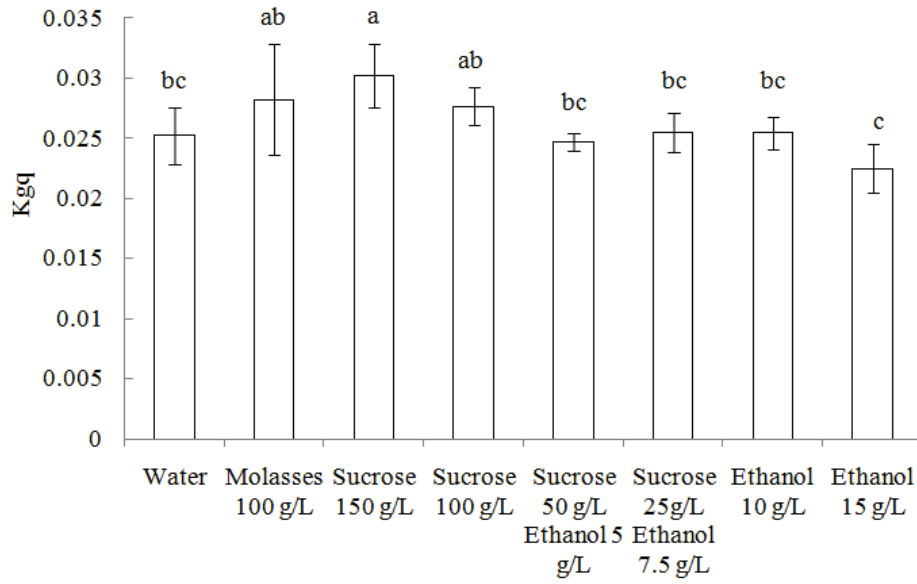
613 **Figure 5.** Comparison between model predictions and measured data in the validation
614 experiment, with L-leucine addition at 12 hours of fermentation. Symbols:
615 experimental measurements, solid lines: model predictions, dotted line: produced
616 isoamyl acetate without considering losses by air stripping.

617 **Figure 6.** Final isoamyl acetate concentration in decane at different concentrations of
618 L-leucine.

619 **Figure 7.a)** Isoamyl acetate distribution in the fermentation-extraction system and
620 losses by stripping for different decane/medium ratios, b) Isoamyl acetate recovery
621 and final concentration in decane at different decane/medium ratios. Results obtained
622 from model simulations.



624 **Figure 1.** Schematic representation of the metabolic pathways involved in isoamyl
 625 acetate synthesis [32].



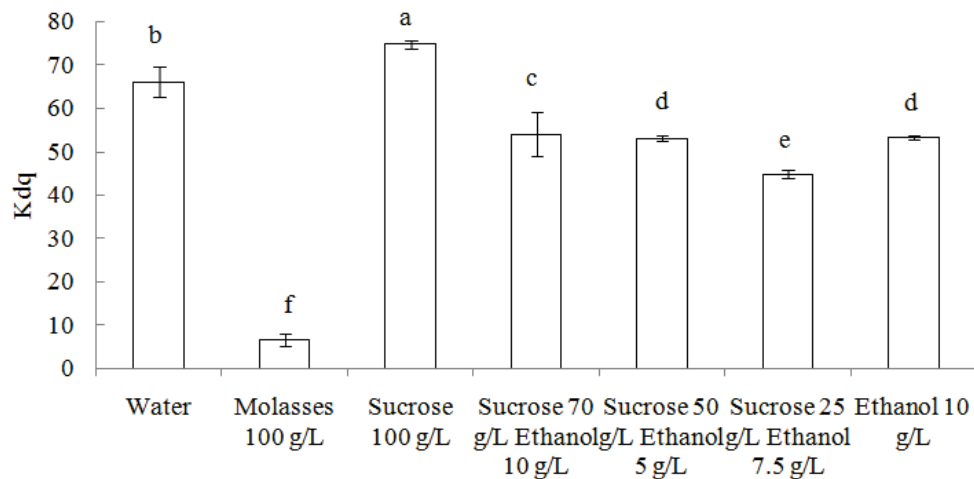
626

627 **Figure 2.** Gas-aqueous phase partition coefficient (K_{gq}) values of isoamyl acetate for

628 different fermentation medium compositions. Error bars represent standard deviation

629 (n=2), different letters correspond to significantly different values.

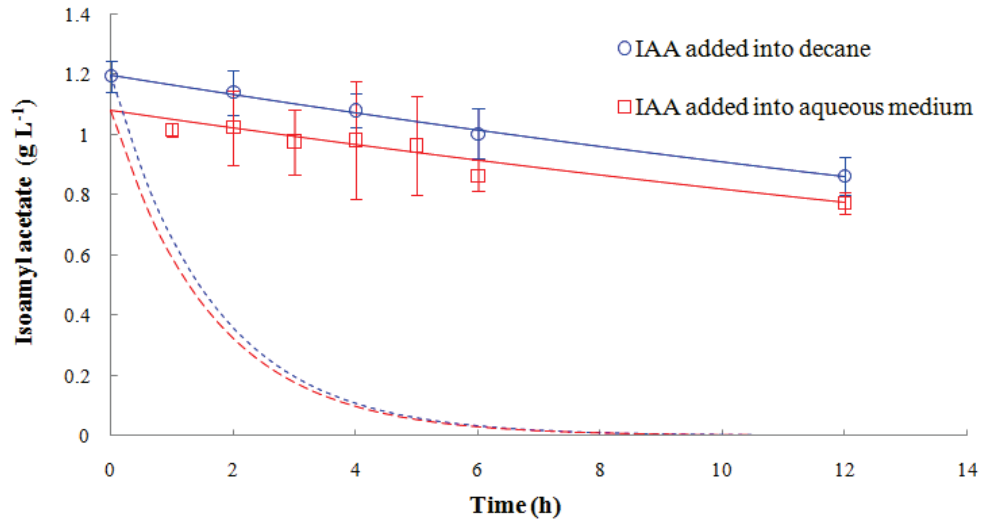
630



631

632 **Figure 3.** Decane–aqueous phase partition coefficient (K_{dq}) values of isoamyl acetate
 633 for different fermentation medium compositions. Error bars represent standard
 634 deviation (n=2), different letters correspond to significantly different values.

635

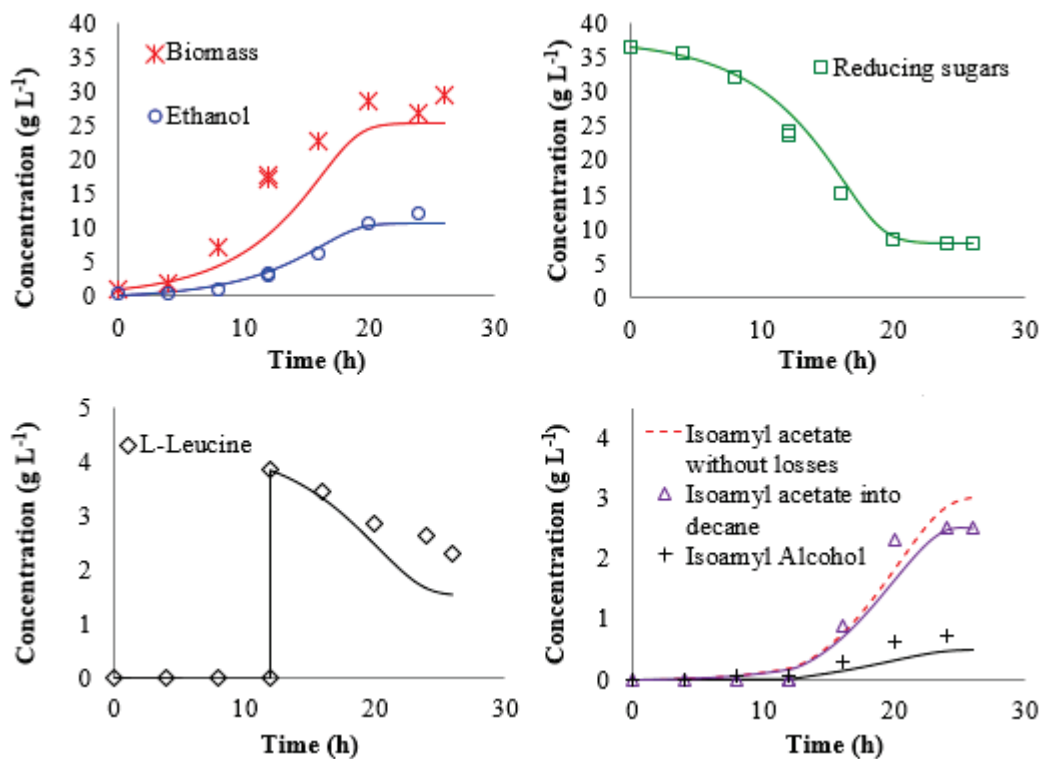


636

637 **Figure 4.** Isoamyl acetate stripping due to air flow. Symbols correspond to
 638 experimental measurements and error bars represent standard error (n=2). Solid lines
 639 represent model predictions considering gas-liquid mass transfer resistance; dashed
 640 lines represent model predictions assuming gas and liquid phases in equilibrium.

641

642



643

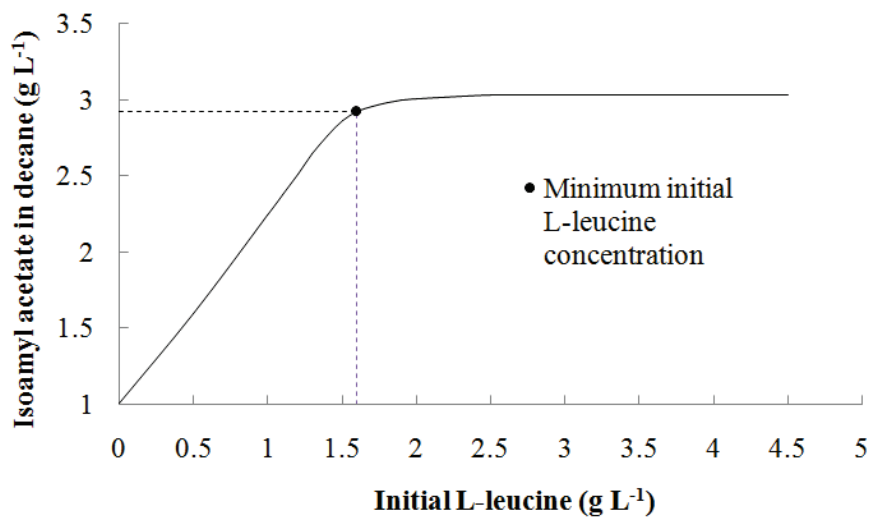
644 **Figure 5.** Comparison between model predictions and measured data in the validation

645 experiment, with L-leucine addition at 12 hours of fermentation. Symbols:

646 experimental measurements, solid lines: model predictions, dotted line: produced

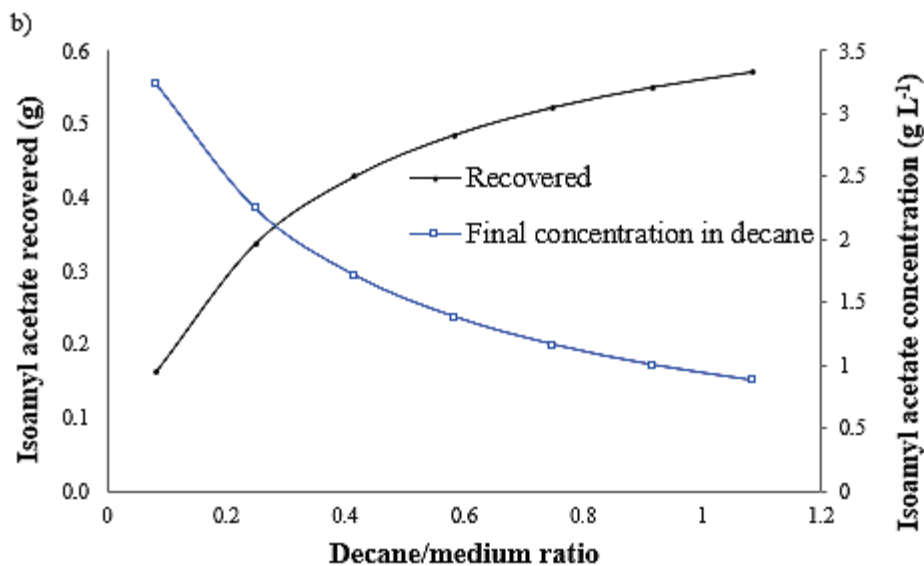
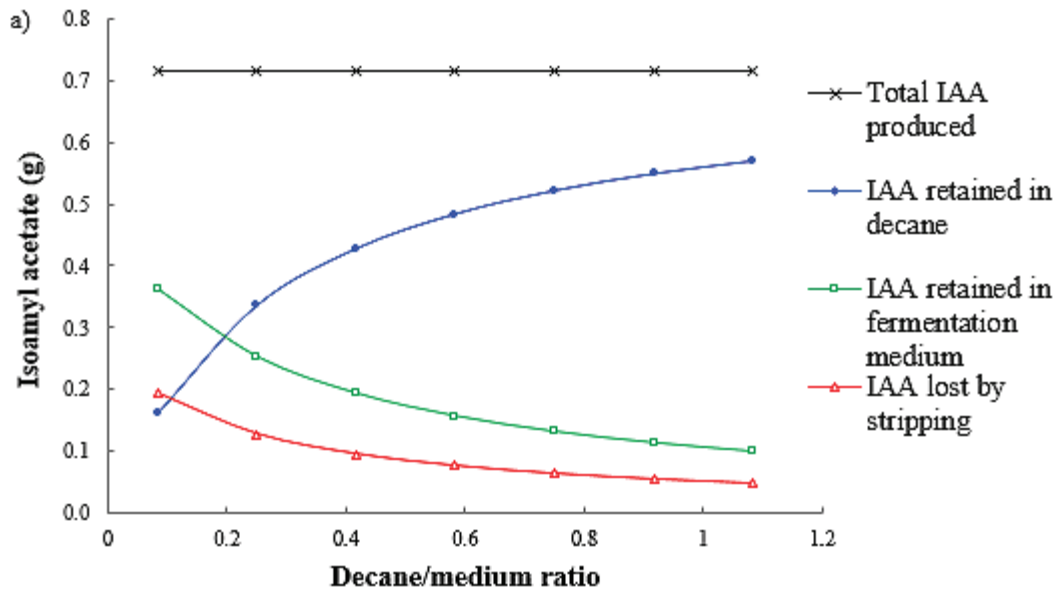
647 isoamyl acetate without considering losses by air stripping.

648



649

650 **Figure 6.** Final isoamyl acetate concentration in decane predicted by the model for
651 different initial concentrations of L-leucine.



652

653 **Figure 7.** a) Isoamyl acetate distribution in the fermentation-extraction system and
 654 losses by stripping for different decane/medium ratios, b) Isoamyl acetate recovery
 655 and final concentration in decane at different decane/medium ratios. Results obtained
 656 from model simulations.

657

Table 1. Mass balance and kinetic equations for the fermentation model, without considering isoamyl acetate extraction by decane and losses by stripping

Compounds	Equations
Biomass	$\frac{dX}{dt} = \mu X \quad (14)$
Ethanol	$\frac{dEtOH}{dt} = \frac{Y_{EtOH/S}}{Y_{X/S}} \mu X \quad (15)$
Isoamyl alcohol	$\frac{dIAOH}{dt} = \xi_S X + \xi_L X - \frac{1}{Y_{IAA/IAOH}} \nu X \quad (16)$
Isoamyl acetate	$\frac{dC}{dt} = \nu X \quad (17)$
Fermentable reducing sugars	$\frac{dS_f}{dt} = -\frac{1}{Y_{X/S}} \mu X \quad (18)$
Leucine	$\frac{dL}{dt} = -\frac{1}{Y_{IAOH/L}} \xi_L X \quad (19)$
Kinetic parameters	Equations
Specific growth rate	$\mu = \mu_{max} \frac{S_f}{K_S + S_f} \quad (20)$
Specific isoamyl alcohol production rate (with sugar consumption)	$\xi_S = \xi_{Smax} \frac{S_f}{K_{SIA} + S_f} \quad (21)$
Specific isoamyl alcohol production rate (with L-leucine consumption)	$\xi_L = \xi_{Lmax} \frac{L}{K_L + L} \frac{S_f}{K_{SIA} + S_f} \quad (22)$
Specific isoamyl acetate production rate	$\nu = \nu_{max} \frac{IAOH}{K_{IAOH} + IAOH} \frac{S_f}{K_{SIA} + S_f} \quad (23)$

658

659

Table 2. Parameter values for isoamyl acetate partition coefficient in the fermentation system.

Partition coefficient	Parameter	Factor	Value \pm standard error
Gas-liquid	p_1	-	-3.716 \pm 0.026
	p_2	S_t	0.0014 \pm 0.0004
	p_3	E	0
	p_4	$S_t E$	0
	p_5	M	0
Liquid-liquid	p_a	-	4.211 \pm 0.083
	p_b	S_t	0
	p_c	E	-0.031 \pm 0.012
	p_d	$S_t E$	0
	p_e	M	-2.326 \pm 0.145

660

661

Table 3. Model parameters and experimental initial conditions

Parameters	Value± standard error			Unit
μ_{max}	0.230 ± 0.006			h^{-1}
ξ_{Smax}	0.0013 ± 0.0003			h^{-1}
ξ_{Lmax}	0.0046 ± 0.0005			h^{-1}
ν_{max}	0.0062 ± 0.0004			h^{-1}
$Y_{X/S}$	0.854 ± 0.050			$g\ g^{-1}$
$Y_{EtOH/S}$	0.373 ± 0.020			$g\ g^{-1}$
$Y_{IAOH/L}$	0.452 ± 0.055			$g\ g^{-1}$
$Y_{IAA/IAOH}$	130/88			$g\ g^{-1}$
K_S	6.41 ± 0.57			$g\ L^{-1}$
K_{SIA}	0.02			$g\ L^{-1}$
K_L	0.02			$g\ L^{-1}$
K_{IAOH}	0.02			$g\ L^{-1}$
$k_t a_t$	0.0117 ± 0.0003			h^{-1}
Initial conditions	1) No addition	2) Addition at t_0	3) Addition at t_{12}	
X_0	0.86 ± 0.12	0.89 ± 0.04	1.01 ± 0.01	$g\ L^{-1}$
S_0	35.18 ± 0.53	32.24 ± 1.88	36.40 ± 1.03	$g\ L^{-1}$
L_0	0.0093	4.03 ± 0.02	0.0093	$g\ L^{-1}$
$EtOH_0$	0.21 ± 0.03	0.17 ± 0.02	0.23 ± 0.05	$g\ L^{-1}$
$IAOH_0$	0	0	0	$g\ L^{-1}$
C_{d0}	0	0	0	$g\ L^{-1}$